Asian Journal of Chemistry; Vol. 26, No. 7 (2014), 1960-1964

ASIAN JOURNAL OF CHEMISTRY

http://dx.doi.org/10.14233/ajchem.2014.15586

Preparation and Microwave Absorbing Property of Dendritic Fe_xCo_{1-x} Alloys

LIANGLIANG TIAN*, FEI WANG, BITAO LIU and YANHUA CAI

Department of Research Center for Materials Interdisciplinary Science, Chongqing University of Arts and Sciences, Chongqing, P.R. China

*Corresponding author: E-mail: tianll07@163.com

Received: 5 April 2013; *Accepted*: 30 October 2013; *Published online*: 22 March 2014; AJC-14936

Dendritic Fe_xCo_{1-x} (x = 0.1, 0.2, 0.3, 0.4, 0.5) alloys were synthesized by low temperature hydrothermal method. Morphology, composition, structure, magnetic property and microwave absorbing property of the Fe_xCo_{1-x} alloys were characterized by scanning electron microscopy, energy disperse spectroscopy, X-ray diffraction, vibrating sample magnetometer and vector network analyzer, respectively. It was found that the composition of the Fe_xCo_{1-x} alloys conforms to the stoichiometric ratio. X-ray diffraction patterns reveal that the alloys show mixed structure when Fe content is lower than 0.3. However, when Fe content is higher than 0.3, the alloys show only bcc structure. The saturation magnetization (M_s) increases and coercivity (H_c) decreases with the increase of the Fe content. The microwave absorbing measurements reveal that the minimum reflection loss of $Fe_{0.1}Co_{0.9}$ alloy is -17.8 dB at 6.4 GHz with a thickness of 2.5 mm, showing the best microwave absorbing property among all the obtained alloys.

Keywords: FeCo alloys, Microwave absorbing property, Permittivity, Permeability.

INTRODUCTION

In recent years, electromagnetic interference pollution has become a problem due to the wide application of electromagnetic systems, radar system[1-4]. In order to solve the problem, microwave absorption materials have attracted lots of attention. Various materials were prepared as microwave absorption materials, such as ferrite[5,6], CuO[7], carbon fiber[8]. With the development of nanotechnology, nanomaterials with different morphologies were synthesized, such as rod-like[9,10], flower-like[11,12], needle-like[13,14] and flake-like[15,16]. It is known that properties of the nanomaterials are influenced by their morphology and thus, microwave absorbing properties may also be affected by the morphology of the materials. It is important to study the influence of morphology on the microwave absorbing property.

Magnetic metals (Fe, Co and Ni) and their composites possess excellent microwave absorbing properties because of the strong attenuation caused by dielectric loss and magnetic loss[17-20]. Feng and Qiu[21] reported Fe-50 wt. % Ni alloys as microwave absorbing materials, showing that morphology of the FeNi alloy changed from spherical to flaky with the increase of the milling time. Simultaneously, the microwave absorbing property enhanced. FeCo alloy and their composite materials were reported as excellent microwave absorbing materials. On the basis of above discussion, microwave absorbing properties of the FeCo alloy can be strongly influenced by their morphology. Fe_3Co_2 nanopowders were synthesized by mechanical alloying and microwave property was found to be dependent of the structure and morphology of the particles[22]. Therefore, it is necessary to study the microwave absorbing property of FeCo alloy with different morphology.

In this paper, Fe_xCo_{1-x} alloys with dendritic morphology were synthesized by low temperature hydrothermal method. Microwave absorbing property of the Fe_xCo_{1-x} alloys was tested. It is revealed that the dendritic Fe_xCo_{1-x} alloys possess excellent microwave absorbing property in the range of 0-8 GHz. This kind of dendritic Fe_xCo_{1-x} alloy has potential application in the field of microwave absorption.

EXPERIMENTAL

All chemicals are of analytical grade and used as received (Sinopharm Chemical Reagent limited corporation). Fe_xCo_{1-x} alloys were synthesized by low temperature hydrothermal method. In a typical experiment, $FeSO_4·7H_2O$ and $CoCl_2·6H_2O$ were dissolved in 0.1 M cetyltrimethylammonium bromide (CTAB) aqueous solution. Then 10 mL of a 25 M NaOH solution and 4 mL NH_2-$NH_2.H_2O$ were added. The final solution was stirred homogeneously and transferred into a 50 mL reactor. After that, the reactor was placed into a drying oven at 130 °C and kept at 200 °C for 2 h. The reactor was cooled down to room temperature in the air. The products were collected and washed for several times and finally dried for 12 h in vacuum oven at 40 °C. In order to obtain Fe_xCo_{1-x} alloys with different composition, the mole ratio of $FeSO_4·7H_2O$ and $CoCl_2·6H_2O$

in the solution was prepared as 0.1/0.9, 0.2/0.8, 0.3/0.7, 0.4/0.6 and 0.5/0.5. The total concentration of $FeSO_4·7H_2O$ and $CoCl_2·6H_2O$ was kept as 0.1 M.

The reduction process of Fe^{2+} and Co^{2+} can be expressed as follows:

$$2Fe^{2+} + N_2H_4 + 4OH^- = 2Fe + N_2 + 4H_2O \quad (1)$$

$$2Co^{2+} + N_2H_4 + 4OH^- = 2Co + N_2 + 4H_2O \quad (2)$$

Detection method: In order to measure microwave property, Fe_xCo_{1-x}/paraffin composite samples were prepared by uniformly mixing the Fe_xCo_{1-x} alloy and paraffin matrix. The composites were compacted into ring shape with 7 mm outer diameter and 3.04 mm inner diameter. The reflection loss (RL) of microwave absorption material can be calculated by the following equations:

$$R = 20\log\left|\frac{Z_I - Z_0}{Z_I + Z_0}\right| \quad (3)$$

$$Z_I = \sqrt{\frac{\mu_0\mu}{\varepsilon_0\varepsilon}}\tanh(j2\pi fd\sqrt{\mu_0\mu\varepsilon_0\varepsilon}) \quad (4)$$

$$Z_0 = \sqrt{\frac{\mu_0}{\varepsilon_0}} \quad (5)$$

where Z_I is the input impedance, Z_0 is the free space impedance; d is the thickness of the absorber. c and f is the light velocity and the frequency of microwave, respectively. ε_0 and μ_0 is vacuum permittivity and vacuum permeability, respectively. ε and μ is complex permittivity and complex permeability, respectively. The complex permittivity and complex permeability of the absorber can be expressed as follows:

$$\varepsilon_r = \varepsilon' - j\varepsilon'' \quad (6)$$

$$\mu_r = \mu' - j\mu'' \quad (7)$$

Chemical composition of the Fe_xCo_{1-x} alloys was analyzed by energy disperse spectroscopy (EDS) and the final value was an average of five measurements. The morphology of the alloys was analyzed on a Hitachi S-4800 field emission scanning electron microscope (FESEM). X-ray diffraction (XRD) measurements were performed on a Rigaku D/Max-2400 X-ray diffractometer using Cu K_α radiation (40 kV, 60 mA). Static magnetic properties were characterized by vibrating sample magnetometer (VSM) (Lak Shore 7304). High frequency electromagnetic property was measured using a vector network analyzer (Agilent PNA E8363B).

RESULTS AND DISCUSSION

Composition of the Fe_xCo_{1-x} alloys: Composition of the Fe_xCo_{1-x} alloys is shown in Table-1. It is noted that the composition of the Fe_xCo_{1-x} alloys is consistent with the mole ratio of Fe^{2+} and Co^{2+} in the solution. Therefore, the obtained five samples can be marked as $Fe_{0.1}Co_{0.9}$, $Fe_{0.2}Co_{0.8}$, $Fe_{0.3}Co_{0.7}$, $Fe_{0.4}Co_{0.6}$ and $Fe_{0.5}Co_{0.5}$. The composition of all the obtained Fe_xCo_{x-1} alloys fits the stoichiometric ratio, so indicating the complete reduction of Fe^{2+} and Co^{2+}. In our previous work describing the properties of the Fe_xCo_{x-1} alloy synthesized by electrodeposition, the Fe content resulted to be always higher than that in solution. This was ascribed to the anomalous code position[23].

Structures and morphologies of the Fe_xCo_{1-x} alloys: Fig. 1 shows the XRD patterns of the obtained dendritic Fe_xCo_{1-x} alloys. Structures of the Fe_xCo_{1-x} alloys change with the increase of the Fe content. $Fe_{0.1}Co_{0.9}$ alloy shows mixed phases with hcp, bcc and fcc. With the increase of Fe content in the alloy, hcp and fcc orientation are apparently depressed and bcc orientation turns into stronger. When the Fe content is higher than 0.3, hcp and fcc structures completely disappear. The alloys only show bcc orientation and bcc (110) displays stronger preferred orientation. Simultaneously, the diffraction peaks located at 82.3° and 99.1° corresponding to Fe phase appear. From a deeper inspection, with the increase of the Fe content in the alloys the bcc diffraction peaks slightly shift to low angle direction, indicating the increase of the lattice constant. The radius of Fe is slightly larger than that of Co. With the increase of Fe, the lattice constant tends to larger. The result is consistent with our previous report[23].

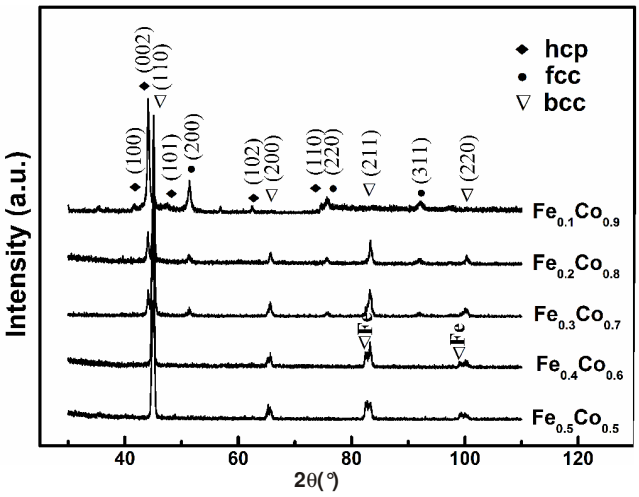

Fig. 1. XRD patterns of the dendritic Fe_xCo_{1-x} alloys

Morphology of the Fe_xCo_{1-x} alloys is shown in Fig. 2. It is found that $Fe_{0.1}Co_{0.9}$ and $Fe_{0.5}Co_{0.5}$ both show dendritic morphology with many branches. The branch of $Fe_{0.1}Co_{0.9}$ is about 1 μm wide and there is a protuberant arris in the axis of the branch. However, branch of $Fe_{0.5}Co_{0.5}$ alloy is different from that of $Fe_{0.1}Co_{0.9}$. The branch of $Fe_{0.5}Co_{0.5}$ alloy shows joints shape.

Magnetic properties of the Fe_xCo_{1-x} alloys: The relationships between Fe content and saturation magnetization (M_s) and coercivity (H_c) of Fe_xCo_{1-x} alloys were measured and displayed

TABLE-1
COMPOSITION OF THE OBTAINED Fe_xCo_{1-x} ALLOYS

Fe^{2+}/Co^{2+}	0.1/0.9	0.2/0.8	0.3/0.7	0.4/0.6	0.5/0.5
Fe (%)	9.71	18.48	31.06	40.94	52.10
Co (%)	90.29	81.52	68.94	59.06	47.90

in Fig. 3. The saturation magnetization (M_s) moves up from 147.5 emu/g to 208.1 emu/g and coercivity (H_c) falls from 134.2 Oe to 68.16 Oe as the Fe content varies from 0.1 to 0.5. Obviously, Fe possesses higher M_s and lower H_c than Co. With the increase of Fe, M_s increases and H_c decreases. From a deeper inspection, it is clear that when the Fe content is lower than 0.3, M_s sharply increases and H_c decreases slowly. However, when the Fe content is greater than 0.3, M_s increases slowly and H_c sharply decreases. From Fig. 1, when the Fe content is lower than 0.3, structure of the alloys shows mixed phases. When the Fe content is greater than 0.3, structure of the alloys is single phase of bcc. Compared with the results shown in Fig. 3, it is indicated that structure of the alloys shows great impact on M_s. However, H_c is strongly influenced by the composition of the alloys.

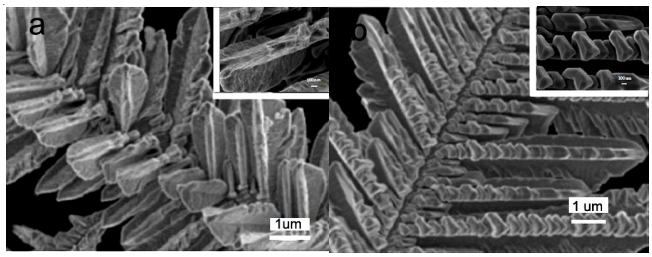

Fig. 2. SEM images of the obtained dendritic Fe_xCo_{1-x} alloys. (a) $Fe_{0.1}Co_{0.9}$ (b) $Fe_{0.5}Co_{0.5}$; Insets of (a) and (b) are the corresponding images of $Fe_{0.1}Co_{0.9}$ and $Fe_{0.5}Co_{0.5}$ with high magnification

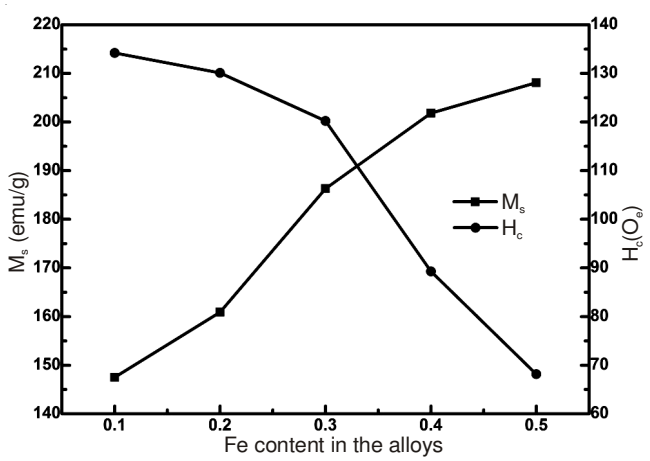

Fig. 3. Dependence of saturation magnetization (M_s) and coercivity (H_c) of the Fe_xCo_{1-x} alloys on the Fe content

Microwave absorbing properties of the Fe_xCo_{1-x} alloys: Generally speaking, microwave absorption mechanism of the absorber can be explained by dielectric loss and magnetic loss. In order to investigate the intrinsic reasons of microwave absorption property, the complex permittivity and permeability of the Fe_xCo_{1-x} were measured in the range of 0-8 GHz. As can be seen from Fig. 4a, the value of ε′ is between 8 and 18 and ε′ decreases with the increase of the Fe content in the alloys. In addition, when the Fe content is lower than 0.3, ε′ sharply decreases. However, when the Fe content is greater than 0.3, ε′ slowly decreases. This change may be explained by the change of structure and composition. As can be seen from Fig. 4b, ε″ value is between 0.25 and 2.5 and the change of ε″ is not so regular. ε″ of $Fe_{0.1}Co_{0.9}$ and $Fe_{0.2}Co_{0.8}$ increases with the increase of frequency. However, ε″ of the other alloys decreases with the increase of frequency. Moreover, there is a wide peak at about 5.0 GHz.

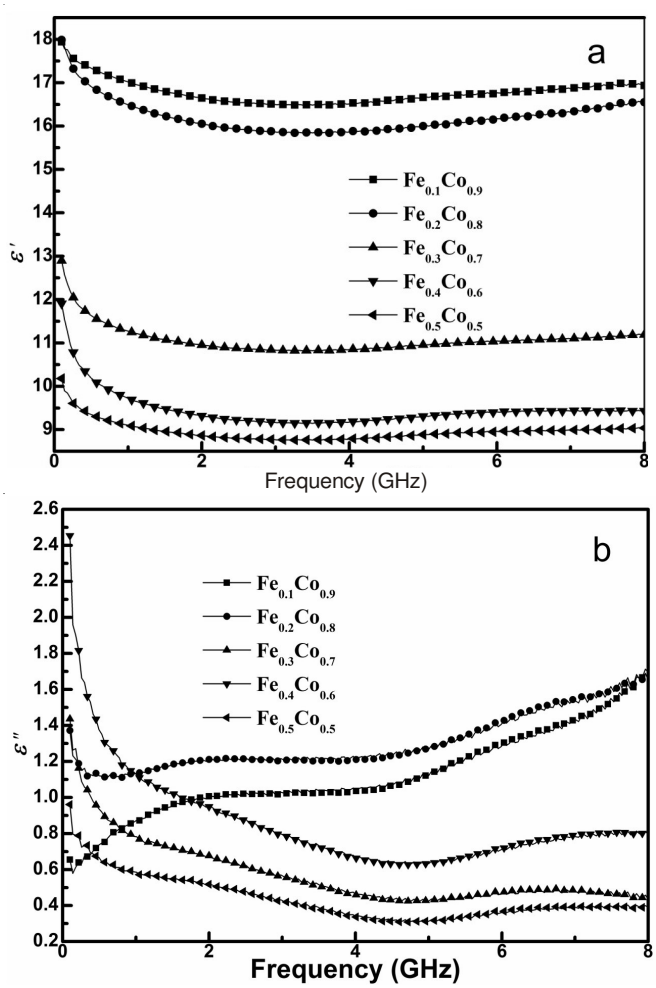

Fig. 4. Complex permittivity of the dendritic Fe_xCo_{1-x} alloys. (a) ε′; (b) ε″

Fig. 5 displays the complex permeability of the Fe_xCo_{1-x} alloys. It is observed that the value of μ′ is between 1.2 and 2.8. μ′ of all the samples is larger in low frequency area. μ″ of the samples is very close and there are two wide peaks located at 0.86 GHz and 5.12 GHz. The peak located at 0.86 GHz corresponds to the consistent natural resonance peak and the peak located at 5.12 GHz can be attributed to the exchange resonance peak. Moreover, μ″ of $Fe_{0.1}Co_{0.9}$ is much higher than the other samples.

Microwave absorbing property of the Fe_xCo_{1-x} alloys within 0-8 GHz was measured and pictured in Fig. 6 and the statistical data was listed in Table-2. According to Eqn. 3-5, when the reflection loss is -10 dB the attenuation of microwave absorption materials achieves 90 %. It is obvious that $Fe_{0.4}Co_{0.6}$ and $Fe_{0.5}Co_{0.5}$ possess general microwave property and the reflection coefficient is always higher than -10 dB, indicating that the absorption of the microwave is lower than 90 %. The reflection coefficient of $Fe_{0.3}Co_{0.7}$ is lower than -10 dB within a small range of 7.7-8.0 GHz with a thickness 2.5 mm. However, $Fe_{0.1}Co_{0.9}$ and $Fe_{0.2}Co_{0.8}$ show excellent microwave absorbing property. The reflectivity of $Fe_{0.1}Co_{0.9}$ is smaller than -10 dB with all the thickness in the range of 2.4-8.0 GHz. The reflec-

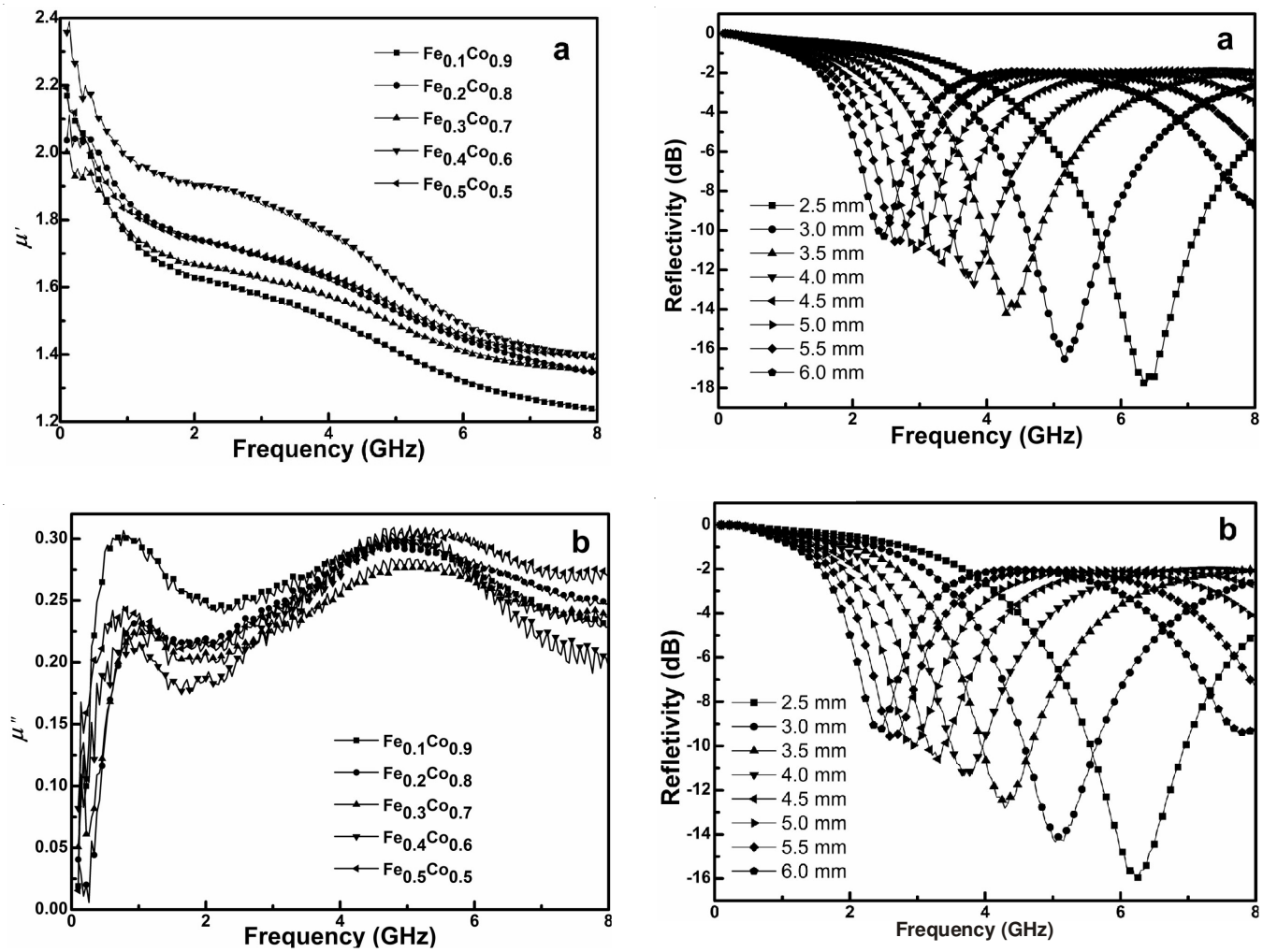

Fig. 5. Complex permeability of the dendritic Fe_xCo_{1-x} alloys. (a) μ′; (b) μ″

tivity of $Fe_{0.2}Co_{0.8}$ is smaller than -10 dB with the thickness 2.5-4.5 mm in the range of 3.2-8.0 GHz. In addition, the reflectivity decreases and the thickness of minimum reflection loss increases with the increase of the Fe content. The frequency of minimum reflection loss first decreases, showing a minimum value 5.1 and then increase to 5.9. As can be seen from Fig. 6a, the reflectivity increases with the thickness increasing. In conclusion, the minimum reflection loss of the Fe_xCo_{1-x} alloys is -17.8 dB at 6.4 GHz with a thickness 2.5 mm.

Conclusion

Dendritic Fe_xCo_{1-x} alloys were successfully synthesized by low temperature hydrothermal method. Fe content in the alloys equals to the Fe^{2+} concentration in the solution. The structure of the alloys is correlated with the composition. It is

TABLE-2
MICROWAVE ABSORBING PROPERTY OF THE Fe_xCo_{1-x} ALLOYS

x	Frequency area (GHz) (RL < -10 dB)	Thickness area (mm) (RL < -10 dB)	Minimum RL (dB)	Frequency of minimum RL (GHz)	Thickness of minimum RL (mm)
0.1	2.4-8.0	2.5-6.0	-17.8	6.3	2.5
0.2	3.2-8.0	2.5-4.5	-16.2	6.2	2.5
0.3	7.7-8.0	2.5	-10.1	5.1	2.5
0.4	None	None	-9.2	5.8	3.0
0.5	None	None	-9.1	5.9	3.0

RL = Reflection loss

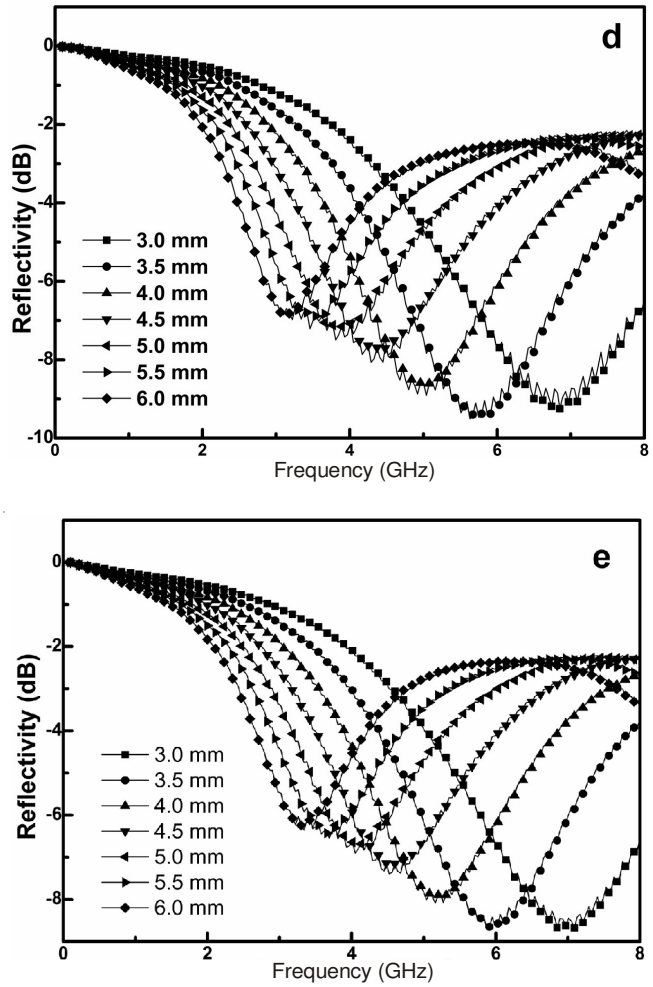

Fig. 6. Reflectivity curves of the Fe_xCo_{1-x} alloys with different thickness. (a) $Fe_{0.1}Co_{0.9}$; (b) $Fe_{0.2}Co_{0.8}$; (c) $Fe_{0.3}Co_{0.7}$; (d) $Fe_{0.4}Co_{0.6}$; (e) $Fe_{0.5}Co_{0.5}$

revealed that the saturation magnetization (M_s) moves up from 147.5 emu/g to 208.1 emu/g and coercivity (H_c) falls from 134.2 Oe down to 68.16 Oe as the Fe content varies from 0.1 to 0.5. The microwave absorbing results show that the minimum reflection loss of the Fe_xCo_{1-x} alloys is -17.8 dB at 6.4 GHz with a thickness 2.5 mm.

ACKNOWLEDGEMENTS

This research was supported by the Foundation of Chongqing Education Commission (KJ121213), Talent Introduction Foundation of Chongqing University of Arts and Sciences (R2012cl14) and Foundation of Chongqing University of Arts and Sciences (Z2011XC15).

REFERENCES

1. I. Cuinas, A.V. Alejos and M.G. Sánchez, *Electron. Lett*., **41**, 340 (2005).
2. A. Balmori, *Pathophysiology*, **16**, 191 (2009).
3. T. Zou, C. Shi and N. Zhao, *J. Mater. Sci*., **42**, 4870 (2007).
4. R. Azaro, S. Caorsi, M. Donelli and G. Gragnani, *Microw. Opt. Technol. Lett*., **28**, 289 (2001).
5. J. Kim and S. Kim, *J. Alloys Comp*., **509**, 4399 (2011).
6. A. Tadjarodi, R. Rahimi, M. Imani, H. Kerdari and M. Rabbani, *J. Alloys Comp*., **542**, 43 (2012).
7. J. Zeng and J. Xu, *J. Alloys Comp*., **493**, L39 (2010).
8. M. Zeng, J. Liu, Y.B. Qin, H.X. Yang, J.Q. Li and J.Y. Dai, *Thin Solid Films*, **520**, 6446 (2012).
9. J. Choma, D. Jamiola, P. Nyga and M. Jaroniec, *Colloids Surf*., **393**, 37 (2012).
10. S. Rong, Z. Ji, Y. Zhu and J. Zhang, *Nonferrous Met. Soc. China*, **18**, 388 (2008).
11. L. Pei, Y. Yang, Y. Pei and S. Ran, *Mater. Charact*., **62**, 1029 (2011).
12. M. Liu, W. Lu, L. Zhao, C. Zhou, H. Li and W. Wang, *Nonferrous Met. Soc. China*, **20**, 2299 (2010).
13. T. You, J. Yan, Z. Zhang, J. Li, J. Tian, J. Yun and W. Zhao, *Mater. Lett*., **66**, 246 (2012).
14. K. Kimura, J. Zhuang, K. Shirabe and Y. Yamashita, *Polymer*, **44**, 4761 (2003).
15. M. Torabi and S.K. Sadrnezhaad, *Curr. Appl. Phys*., **10**, 72 (2010).
16. B.B. Nayak, S.K. Mohanty, M. Takmeel, D. Pradhan and A. Mondal, *Mater. Lett*., **64**, 1909 (2010).
17. Y. Feng and T. Qiu, *J. Alloy. Comp*., **513**, 455 (2012).
18. J. Liu, Y. Feng and T. Qiu, *J. Magn. Magn. Mater*., **323**, 3071 (2011).
19. W. Yang, Y. Fu, A. Xia, K. Zhang and Z. Wu, *J. Alloys Comp*., **518**, 6 (2012).
20. K.-Y. Park, J.-H. Han, S.-B. Lee and J.-W. Yi, *Compos. Part A*, **42**, 573 (2011).
21. Y. Feng and T. Qiu, *J. Magn. Magn. Mater*., **324**, 2528 (2012).
22. P. Zhou, L. Deng, J. Xie and D. Liang, *J. Alloys Comp*., **448**, 303 (2008).
23. C. Qiang, J. Xu, S. Xiao, Y. Jiao, Z. Zhang, Y. Liu, L. Tian and Z. Zhou, *Appl. Surf. Sci*., **257**, 1371 (2010).